Isotope Microscopic Observation of Osteogenesis Process Forming Robust Bonding of Double Network Hydrogel to Bone

Takayuki Nonoyama, Lei Wang, Masumi Tsuda, Yuki Suzuki, Ryuji Kiyama, Kazunori Yasuda, Shinya Tanaka, Kousuke Nagata, Ryosuke Fujita, Naoya Sakamoto, Noriyuki Kawasaki, Hisayoshi Yurimoto, Jian Ping Gong**

((Optional Dedication))

Dr. T. Nonoyama, Prof. K. Yasuda, Prof. J. P. Gong
Faculty of Advanced Life Science, Hokkaido University, Kita-21 Nishi-11, Kita-ku, Sapporo 001-0021, Japan
E-mail: nonoyama@sci.hokudai.ac.jp, gong@sci.hokudai.ac.jp

Dr. L. Wang, Dr. M. Tsuda, Prof. S. Tanaka
Department of Cancer Pathology, Faculty of Medicine, Hokkaido University, Kita-15, Nishi-7, Kita-ku, Sapporo 060-8638, Japan

Dr. T. Nonoyama, Prof. K. Yasuda, Prof. J. P. Gong, Dr. L. Wang, Dr. M. Tsuda, Prof. S. Tanaka
Global Station for Soft Matter, Global Institution for Collaborative Research and Education (GI-CoRE GSS), Hokkaido University, Kita-21 Nishi-11, Kita-ku, Sapporo 001-0021, Japan

Prof. J. P. Gong, Prof. S. Tanaka
Institute for Chemical Reaction Design and Discovery (WPI-ICReDD), Hokkaido University, Kita-21 Nishi-11, Kita-ku, Sapporo 001-0021, Japan

Y. Suzuki, R. Kiyama
Graduate School of Life Science, Hokkaido University, Kita-21 Nishi-11, Kita-ku, Sapporo 001-0021, Japan

Dr. K. Nagata, Dr. N. Kawasaki, Prof. H. Yurimoto
Department of Natural History Sciences, Hokkaido University, Kita-21 Nishi-11, Kita-ku, Sapporo 001-0021, Japan

Dr. R. Fujita, Dr. N. Sakamoto
Isotope Imaging Laboratory, Creative Research Institution, Hokkaido University, Kita-21 Nishi-11, Kita-ku, Sapporo 001-0021, Japan

Dr. R. Fujita
Laboratory of Sanitary Entomology, Faculty of Agriculture, Kyushu University, Motooka 744, Nishi-ku, Fukuoka 819-0395, Japan

Keywords: Tough Hydrogel, Hydroxyapatite, Osteogenesis, Bone Absorbable Materials, Isotope Microscopy

Abstract

Tough double network (DN) hydrogels are promising substitutes of soft supporting tissues such as cartilage and ligaments. For such applications, it is indispensable to robustly fix the hydrogels to bones with medically feasible methods. Recently, we succeeded in robustly bonding the DN hydrogels to defected bones of rabbits *in vivo*. The osteo-conductance was achieved by mineralizing in the surface layer of the DN hydrogels with calcium-phosphate-hydroxide salt hydroxyapatite (HAp) nano crystals of low crystallinity. Spontaneous osteogenesis penetrating into the semi-permeable hydrogels occurs to form a gel/bone composite layer of 40 μm-thick within four weeks after the implantation. In this work, we implanted the ^{44}calcium isotope-doped HAp/DN hydrogel in a defect of rabbit femoral bone, and analyzed the dynamic osteogenesis process at the gel/bone interface by tracing the calcium isotope ratio $^{44}Ca/^{40}Ca$ using isotope microscopy. The synthetic HAp hybridized on the surface layer of DN gel dissolves rapidly in the first two weeks by inflammation, and then the immature bone with a gradient structure starts to form in the gel region, reutilizing the dissolved Ca ions. These results reveal, for the first time, that HAp hybridized in the DN hydrogel is reutilized for the osteogenesis to form the bone/gel composite layer at the gel/bone interface. These facts also help to understand the lifetime of bone absorbable materials and to elucidate the mechanism of spontaneous, non-toxic, but strong fixation of hydrogels to bones.

Main text

Hydrogels, a class of soft materials storing a large amount of water in three-dimensional polymeric network, possess flexibility, low friction and high permeability of small molecules and ions. Owing to the recent development of several strategies to toughen the soft materials, many hydrogels have acquired sufficiently high strength and toughness as load-bearing structural biomaterials [1-4]. Double network (DN) hydrogels, a representative in the class of tough hydrogels, possess modulus, strength, and toughness that are comparable to those of

cartilages while containing ~90 wt% water [1,2]. The invention of tough and strong hydrogels provides novel strategies to treat injured component tissues of human joint, such as articular cartilage, meniscus, and ligament, using various artificial tissues and implants to induce tissue regeneration [5-7]. For example, localized replacement of only the injured articular cartilage with the artificial cartilage would provide a potential surgical option, which is less invasive than the currently available total joint replacement using hard metallic or sintered ceramics components [8]. To apply hydrogel materials for artificial cartilage applications, a robust fixation to bone tissue is indispensable. However, it is extremely challenging to establish a non-toxic and medically feasible method because no glues work well on such a watery surface of hydrogels. Calcium phosphate salts such as low-crystalline hydroxyapatite (HAp) and β-tricalcium phosphate (β-TCP) have been applied to promote bone regeneration as bone absorbable materials because of their excellent bio-absorbable and osteoconductive properties [9,10]. Recently, we developed a technique to make a robust fixation of DN gel to bone tissues *in vivo*. The technique is by mineralizing low-crystalline HAp nanoparticles with ~600 nm diameter to the surface layer of the semi-permeable DN hydrogel [11-15]. When HAp-hybridized DN gel is implanted in a defect created in bones, the HAp induces osteogenesis penetrating into the gel matrix, which forms the strong bonding of the DN gel to bone within 4 weeks. On the other hand, the pristine DN gel without HAp-hybridization did not show any bonding to bone at all even after 12 weeks implantation. This technique provides a general, non-toxic, and medically feasible approach to form robust fixation of the semi-permeable DN hydrogels to bones by the formation of gel/bone composite layer.

In this work, we intend to clarify the dynamic process of HAp-induced osteogenesis penetrating into the DN gel matrix, which results in the robust fixation of gel to bone tissue. We focus on the reutilization of the synthetic HAp during the osteogenesis process. Generally, at the early stage of the bone reconstruction process, chondrocytes construct extracellular matrix (ECM) composed of collagen and proteoglycan at the defect, and then chondrocytes

secrete alkaline phosphatase to mineralize HAp from body fluid in the ECM. After that, osteoblasts penetrate into the mineralized ECM with the construction of blood vessel and produce immature woven bone [16,17]. This bone is subsequently deconstructed by osteoblast-induced osteoclast, and then osteoblast remodels functionalized mature bone. In the presence of the bone absorbable materials, it has been generally accepted that such material is dissolved to calcium and phosphate ions by osteoclast and then reutilized to construct bone tissue by osteoblast in the osteogenesis process [18,19]. However, direct evidence to prove the reutilization has not been obtained because both synthetic calcium phosphate implants and bone tissues are made of the same inorganic compound and cannot be distinguished at all. Currently, the only evidence of the "resorbable" is that the material disappears from the implantation location over time [20].

To reveal the HAp reutilization, isotope analysis is a strong solution. Yurimoto et al. have developed isotope microscopy, based on the secondary ion mass spectrometry, to evaluate not only geological minerals and meteorites in cosmic science [21-23] but also biominerals [24, 25]. In this work, we apply this unique and powerful technique to analyze the HAp reutilization in osteogenesis process at the bone-gel interface. When a HAp/DN hydrogel with isotope-anomalous calcium phosphate salt is implanted in the defect of bone that possesses natural isotope ratio, the implant and tissue can be distinguished based on isotope ratio, and then the reutilization of implant HAp in the osteogenesis should be evaluated by tracing the isotope ratio of regenerated bone. In this study, we implanted the DN hydrogels containing isotope anomalous HAp nanoparticles in the defected femoral trochlea of the patellofemoral joint of rabbits, and the time and spatial evolutions of the isotope anomaly were observed. For the first time, we identified the reutilization of synthetic HAp implant during the osteogenesis. This work strongly supports our previously reported explanation that the dissolution and diffusion of a small amount of HAp nanocrystals stimulate the cells on the bone region to perform osteogenesis forming the gel/bone layer. This work also gives important insight into

understanding the bone regeneration process induced by other implanted materials, which is beneficial for the design and development of novel bone-resorbable materials.

Figure 1 shows the schematic illustration of the experimental procedures to prepare the ^{44}HAp/DN gel (**Figure 1a**), to implant and evaluate the reutilization of the implanted HAp in the osteogenesis *in vivo* (**Figure 1b**). The cylindrical DN gel plug with ^{44}HAp nanoparticles hybridized in the surface layer of its sidewall was implanted in the osteochondral defect created in the rabbit femoral groove of the bilateral patellofemoral joints. The ^{44}HAp/DN gel implant with surrounding cancellous bone tissue was harvested at 2, 4, 6 and 12 weeks after the surgery, and the 14 μm-thick sections in transverse plane processed by using cryostat under frozen temperature were placed on the silicon wafer. The defrosted and dried slice was coated by gold evaporation. The boundary between ^{44}HAp/DN gel and cancellous bone of rabbit was observed by the isotope microscope.

The optical microscopic images of the slice specimen showed the center circle region of ^{44}HAp/DN gel plug and surrounding cancellous bone (**Figure 2**). An obvious gap between gel and bone, indicated by red arrow in the figure, was observed at 2 weeks (**Figure 2a-i**). A minor connection between gel and bone, indicated by red arrow in the figure, was observed at 4 weeks (**Figure 2b-i**). The gap was hardly observed and most of the interface was connected at 6 weeks (**Figure 2c-i**). The interface was connected completely at 12 weeks (**Figure 2d-i**). No large gap was observed at the sample harvest even for 2 and 4-week samples because the gel plug with 4.5-mm diameter was press-fitted in the created defect (4.3 mm of inner diameter). The gap appeared in the drying process of slice due to less adhesion of ^{44}HAp/DN gel plug to bone tissue at the boundary. The ^{44}HAp coating region became unclear with increasing implantation period, indicating dissolution and diffusion of HAp over time.

The key parameter of this study is the ratio of target isotope ^{44}Ca to major ^{40}Ca (^{44}Ca/^{40}Ca). The atomic fractions of ^{40}Ca and ^{44}Ca in nature are 96.94% and 2.086%, respectively [26], which gives the natural isotope ratio ^{44}Ca/^{40}Ca of 0.022. On the other hand,

$^{44}Ca/^{40}Ca$ of the prepared ^{44}HAp is calculated as 0.132 considering the mixing ratio of $^{44}CaCl_2$ and $^{nat}CaCl_2$ (1 : 9 = $^{44}CaCl_2$: $^{nat}CaCl_2$) and purity of isotope reagent (^{40}Ca 2.89%, ^{44}Ca 97.00%) (**Supporting Experimental Section**).

First, we measured the values of $^{44}Ca/^{40}Ca$ of natural cancellous bone tissue and pristine ^{44}HAp coated DN gel plug. The measurement was performed on the sample implanted at time zero. The isotope images of ^{40}Ca, ^{44}Ca, and $^{44}Ca/^{40}Ca$ for the natural cancellous bone were taken at a position far from the implanted position (**Supporting Figure S1a**). The sponge morphology can be observed from the individual isotope images. The $^{44}Ca/^{40}Ca$ of natural bone tissue calculated from the data points in the black dotted square of the image was 0.020±0.001. Moreover, $^{44}Ca/^{40}Ca$ of ^{44}HAp near the surface of the implanted DN gel was 0.132±0.001, measured by a spot analysis (**Supporting Figure S1b**). The measured $^{44}Ca/^{40}Ca$ values of natural bone (0.020±0.001) and ^{44}HAp/DN gel (0.132±0.001) were well-consistent with the theoretical values.

Next, the isotope images around the boundary between the cancellous bone and the ^{44}HAp/DN gel at 2, 4, 6 and 12 weeks after the implantation are shown in **Figure 2**. The images of all periods were acquired at the connected regions between gel and bone observed in the optical microscopic images, showing by the red squares. The $^{44}Ca/^{40}Ca$ image at 2 weeks (**Figure 2a-iv**) showed a clear border between the gel and bone; Moreover, the ^{44}HAp/DN gel (0.090) was lower than the pristine ^{44}HAp/DN gel (0.132), indicating the dissolution and diffusion of ^{44}HAp. On the other hand, the $^{44}Ca/^{40}Ca$ in the bone region remained the same value (0.020), meaning that the bone facing to the ^{44}HAp/DN gel was the pre-existed tissue, not the regenerated one. Besides, it indicates that the dissolved Ca^{2+} ions from the mineralized HAp did not diffuse into the bone tissue because of the bony solidity. From the relatively homogeneous image, the decrement of $^{44}Ca/^{40}Ca$ due to dissolution and diffusion of Ca^{2+} ions should uniformly occur in the whole gel region (**Figure 2a-iv**). These results indicate that the osteogenesis hardly penetrated the gel region in a short period of 2 weeks. This is consistent

with our previous observation that the adhesion of HAp-coated DN gel to bone at 2 weeks was weak [11,12]. A clear $^{44}Ca/^{40}Ca$ border was still observed at 4 weeks (**Figure 2b-iv**). However, the $^{44}Ca/^{40}Ca$ value of gel near the boundary with ~30 μm thick (white arrowed, 0.073) was slightly lower than that of inner bulk (0.080) in the 4-week image. The slight decrement of gel near the boundary could be associated to the ingrowth of immature bone, as shown by TEM observation in our previous report [11,12]. At 6 weeks after the implantation, the boundary became very diffusive, and the gradient distribution of $^{44}Ca/^{40}Ca$ was observed (**Figure 2c-iv**). This continuous morphology from gel to bone implied that the regenerated bone, which was more mature than that of 4 weeks, penetrated into the gel region. The gradient structure at the boundary became wider in 12 weeks (**Figure 2d-iv**). These results clearly indicate that during the implantation, the ^{44}HAp is gradually dissolved and diffused, and then the osteogenesis propagates into the gel implant to form the robust bonding of gel to bone tissue.

To reveal the reutilization of implant HAp in the osteogenesis, the line profile of $^{44}Ca/^{40}Ca$ around the boundary was further studied. Since the ^{44}HAp was gradually dissolved and diffused, it is difficult to identify the initial boundary between gel and bone from the $^{44}Ca/^{40}Ca$ line profile. Alternatively, we used the sulfur element contained in the PAMPS 1st network of the DN gel to determine the initial boundary. It was confirmed that the DN gel does not degrade in such a short implantation period [27], so the line profile of sulfur should not change with time. **Figure 3a** shows the line profiles of $^{44}Ca/^{40}Ca$ ratio measured by isotope microscopy, and the intensities of calcium and sulfur measured by energy dispersed X-ray spectroscopy (EDS) at the boundary region. The measurement range of line analysis was wider than the imaging analysis of **Figure 2**. Some $^{44}Ca/^{40}Ca$ data of the line profiles at the boundary was failed to collect because of the poor ionization efficiency in the isotope microscopic analysis. The dash lines in the $^{44}Ca/^{40}Ca$ curves were drawn based on the reference to the line profiles generated from mapping image (**Supporting Figure S2**). An abrupt drop in the normalized sulfur intensity (red curves) was observed for all the samples harvested at different

implanted times, which identifies the initial boundary position between the gel and the bone, and was set as zero position in **Figure 3a**. The gel region and the bone region were highlighted in blue and orange colors, respectively. Although the $^{44}Ca/^{40}Ca$ profile (black curve) around the boundary at 2 weeks was not collected (**Figure 3a-i**), we speculate a relatively sharp line profile from the corresponding imaging data (**Figure 2**). The high normalized Ca intensity (blue curve) in the bone region (1.0 to 1.2) than that in the gel region (~0.2) far from the boundary is consistent with the fact that the HAp density of bone was much higher than that of ^{44}HAp in the gel. The $^{44}Ca/^{40}Ca$ ratio was decreased to 0.09 from the initial value (0.132) after 2 weeks. With increasing in the implantation period, the $^{44}Ca/^{40}Ca$ ratio decreased from gel to bone regions, and the gradient width was expanded (**Figure 3a-ii-iv**). Specifically, $^{44}Ca/^{40}Ca$ was decreased inside the gel and saturated at lower values far from the boundary, while $^{44}Ca/^{40}Ca$ out of the gel was increased with the time. These results further confirm the dissolution of ^{44}HAp in the gel and diffusion to outside of the gel. Furthermore, the gradient width of Ca intensity also became expanded with time, but in the opposite direction: the Ca intensity in the gel region increased while that in the bone region decreased slightly at the boundary. The region that both Ca intensity and $^{44}Ca/^{40}Ca$ ratio changed indicates the newly regenerated bone by osteogenesis, which is shown by hatched lines in **Figure 3a**. That is, the right region with 0.020 of the $^{44}Ca/^{40}Ca$ ratio and ~1.2 of Ca intensity was pre-existed bone. In contrast, the hatched region, where both $^{44}Ca/^{40}Ca$ ratio and the Ca intensity were in gradient structure, is where the bone was newly regenerated. After 12 weeks of implantation, the newly formed bone region was about ~ 450 μm-thick (~200 μm inside the gel and ~250 μm outside of the gel), consistent with our previous observation by TEM [11]. From the fact that the $^{44}Ca/^{40}Ca$ ratio located outside of gel matrix is obviously higher than the natural ratio 0.020, the regenerated bone reutilized the HAp, because the isotope anomaly could not come from ingested feeds and reutilization of pre-existed bone. Therefore, this work gives the first direct evidence that the implanted HAp is reutilized to reconstruct bone tissues.

From the time evolution of $^{44}Ca/^{40}Ca$, we can estimate the characteristic time of implanted HAp *in vivo* in the relatively early stage of osteogenesis. **Figure 3b** shows the $^{44}Ca/^{40}Ca$ at a position = -60 μm of line profile as a function of the implantation period. The plots were well-fitted by a simple attenuation function, and the characteristic time of ~16 days was estimated. This characteristic time is well consistent with the period of ~ 14 days for the formation of first immature (woven) bone.

Based on the above results, we present a schematic illustration of the primary bone remodeling with ^{44}HAp/DN gel implant, as shown in **Figure 3c**. After the implantation of HAp/DN gel, the inflammation occurs, which causes HAp dissolution because the environmental pH becomes acidic by inflammation. So, the Ca ions diffuse to surrounding regions at a relatively fast rate in this earliest stage. Over ~14 days, the inflammation subsides, and the HAp dissolution is suppressed. Alternately, the immature bone is formed, which also acts as a physical barrier to prevent further Ca diffusion. Therefore, the decreasing rate of Ca becomes slower after 14 days and then reaches equilibrium over 40 days. After this early period, the reconstruction to the mature bone is dominantly controlled by cellular activities of osteoclast and osteoblast. As a result, newly formed bones penetrated in the gel form a strong bonding between the gel and the bone.

The unique isotope microscopy firstly revealed the reutilization of synthetic HAp implant to osteogenesis *in vivo*. When we implant HAp-coated tough gel in the defect created at the femoral groove, the HAp is chemically dissolved and diffused due to acidic conditions by inflammation at the earliest stage of surgery. After the subside of the inflammatory, the immature woven bone is formed by using ions dissolved from the implant. This woven bone formation penetrates into gel matrix to achieve robust fixation. The dissolution and diffusion of HAp get slow down over 2 weeks because of the physical barrier of woven bone and less inflammation. After this early stage, the reconstruction from woven bone to functional mature bone is performed by the biological reaction of osteoblast and osteoclast. The isotopic analysis

can trace the lifetime and reutilization of HAp implants *in vivo*, so it is a strong tool to evaluate the molecular process of bone-related materials.

Supporting Information

Supporting Information is available from the Wiley Online Library or from the author.

Acknowledgements

This research was financially supported by JSPS KAKENHI (Grant Number 17H06144, JP17H06376). We thank the Open Facility, Global Facility Center of Hokkaido University, for isotope microscopic measurements. The authors thank Prof. Kuniharu Ijiro (Hokkaido University) for precious suggestion on the work. The authors also thank Dr. Masanori Kikuchi (National Institute for Materials Science), Prof. Dr. Chikara Ohtsuki (Nagoya University) and Prof. Dr. Kunio Ishikawa (Kyusyu University) for discussions on the HAp re-utilization.

Received: ((will be filled in by the editorial staff))
Revised: ((will be filled in by the editorial staff))
Published online: ((will be filled in by the editorial staff))

References

[1] J. P. Gong, Y. Katsuyama, T. Kurokawa, Y. Osada, *Advanced Materials* **2003**, *15*, 1155.

[2] J. P. Gong, *Soft Matter* **2010**, *6*, 2583.

[3] K. Ito, *Current Opinion in Solid State and Materials Science* **2010**, *14*, 28.

[4] T. Sakai, T. Matsunaga, Y. Yamamoto, C. Ito, R. Yoshida, S. Suzuki, N. Sasaki, M. Shibayama, U. Il Chung, *Macromolecules* **2008**, *41*, 5379.

[5] K. Yasuda, J. Ping Gong, Y. Katsuyama, A. Nakayama, Y. Tanabe, E. Kondo, M. Ueno, Y. Osada, *Biomaterials* **2005**, *26*, 4468.

[6] K. Yasuda, N. Kitamura, J. P. Gong, K. Arakaki, H. J. Kwon, S. Onodera, Y. M. Chen, T. Kurokawa, F. Kanaya, Y. Ohmiya, et al., *Macromolecular Bioscience* **2009**, *9*, 307.

[7] N. Kitamura, M. Yokota, T. Kurokawa, J. P. Gong, K. Yasuda, *Journal of Biomedical Materials Research Part A* **2016**, *104*, 2159.

[8] K. Arakaki, N. Kitamura, H. Fujiki, T. Kurokawa, M. Iwamoto, M. Ueno, F. Kanaya, Y. Osada, J. P. Gong, K. Yasuda, *Journal of Biomedical Materials Research Part A* **2009**, *93A*, 1160.

[9] T. Furukawa, Y. Matsusue, T. Yasunaga, Y. Shikinami, M. Okuno, T. Nakamura, *Biomaterials* **2000**, *21*, 889.

[10] W. R. Walsh, F. Vizesi, D. Michael, J. Auld, A. Langdown, R. Oliver, Y. Yu, H. Irie, W. Bruce, *Biomaterials* **2008**, *29*, 266.

[11] T. Nonoyama, S. Wada, R. Kiyama, N. Kitamura, M. T. I. Mredha, X. Zhang, T. Kurokawa, T. Nakajima, Y. Takagi, K. Yasuda, et al., *Advanced Materials* **2016**, *28*, 6740.

[12] R. Kiyama, T. Nonoyama, S. Wada, S. Semba, N. Kitamura, T. Nakajima, T. Kurokawa, K. Yasuda, S. Tanaka, J. P. Gong, *Acta Biomaterialia* **2018**, *81*, 60.

[13] S. Wada, N. Kitamura, T. Nonoyama, R. Kiyama, T. Kurokawa, J. P. Gong, K. Yasuda, *Acta Biomaterialia* **2016**, *44*, 125.

[14] T. Nonoyama, *Polymer Journal* **2020**, *52*, 709.

[15] K. Fukao, K. Tanaka, R. Kiyama, T. Nonoyama, J. P. Gong, *Journal of Materials Chemistry B* **2020**, *8*, 5184.

[16] T. A. Einhorn, L. C. Gerstenfeld, *Nature Reviews Rheumatology* **2015**, *11*, 45.

[17] U. Saran, S. Gemini Piperni, S. Chatterjee, *Archives of Biochemistry and Biophysics* **2014**, *561*, 109.

[18] D. Buser, B. Hoffmann, J. Bernard, A. Lussi, D. Mettler, R. K. Schenk, *Clinical Oral Implants Research* **1998**, *9*, 137.

[19] M. Chazono, T. Tanaka, H. Komaki, K. Fujii, *Journal of Biomedical Materials Research* **2004**, *70A*, 542.

[20] M. Bohner, *Materials Today* **2010**, *13*, 24.

[21] H. Yurimoto, K. Nagashima, T. Kunihiro, *Applied Surface Science* **2003**, *203–204*, 793.

[22] K. Nagashima, A. N. Krot, H. Yurimoto, *Nature* **2004**, *428*, 921.

[23] N. Sakamoto, Y. Seto, S. Itoh, K. Kuramoto, K. Fujino, K. Nagashima, A. N. Krot, H. Yurimoto, *Science* **2007**, *317*, 231.

[24] H. Hongo, M.Sasaki, S. Kobayashi, T. Hasegawa, T. Yamamoto, K. Tsuboi, E. Tsuchiya, T. Nagai, N. Khadiza, M. Abe, A. Kudo, K. Oda, P. Henrique Luiz de Freitas, M. Li, H. Yurimoto, N. Amizuka, *Journal of Histochemistry & Cytochemistry*, **2016**, *64*, 601.

[25] N. Hiraishi, S. Kobayashi, H. Yurimoto, J. Tagami, *Dental Materials*, **2018**, *34*, e57.

[26] K. J. R. Rosman, P. D. P. Taylor, *Pure and Applied Chemistry* **1998**, *70*, 217.

[27] C. Azuma, K. Yasuda, Y. Tanabe, H. Taniguro, F. Kanaya, A. Nakayama, Y. M. Chen, J. P. Gong, Y. Osada, *Journal of Biomedical Materials Research Part A* **2007**, *81A*, 373.

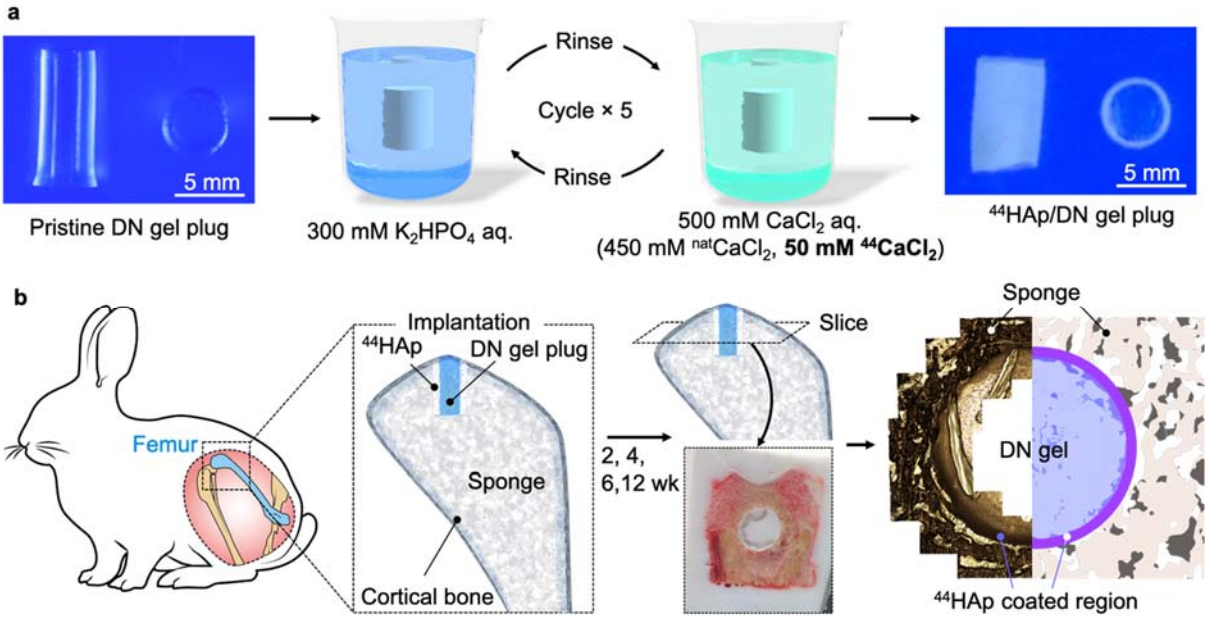

Figure 1. Experimental procedures to prepare the implanted specimens for isotope microscopic observation. (a) The ^{44}HAp coating to the subsurface of DN gel plug by the alternative soaking of K_2HPO_4 aq. and $CaCl_2$ aq. containing 10% $^{44}CaCl_2$. (b) The implantation of ^{44}HAp-coated DN gel into the defected femoral trochlea of the patellofemoral joint of rabbits and the schematic image and optical microscopic image of the sliced specimen in the transverse plane.

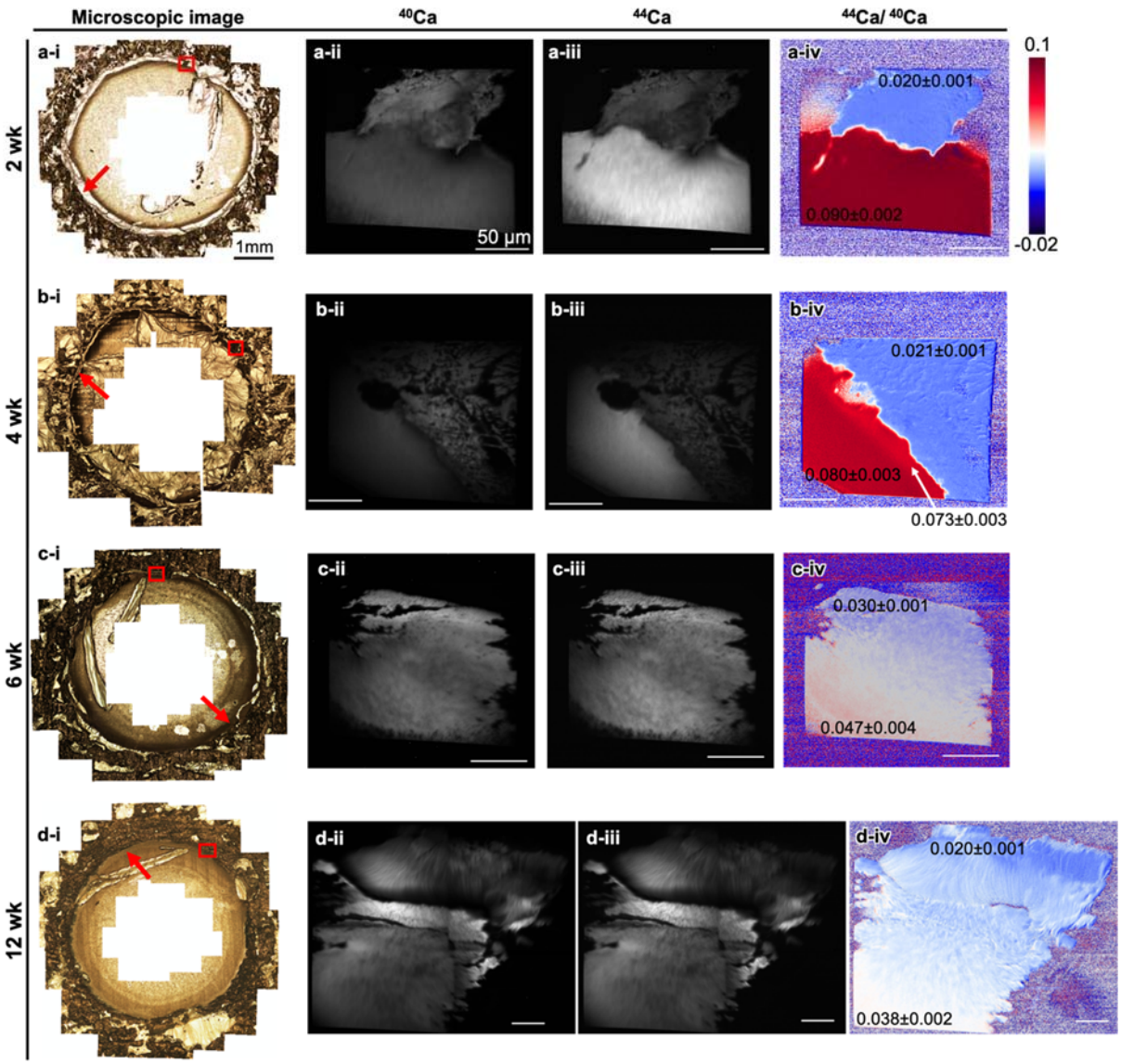

Figure 2. Optical microscopic images and isotope microscopic images. Optical microscopic images **(i)**, raw images of ^{40}Ca **(ii)** and ^{44}Ca **(iii)** mappings, and color mapping of ^{44}Ca/^{40}Ca ratio **(iv)** at 2 **(a)**, 4 **(b)**, 6 **(c)** and 12 **(d)** weeks. Red arrows indicate the boundary between bone and gel. Isotope images **(ii to iv)** were acquired at the red squares. The global optical microscopic images of the implanted ^{44}HAp/DN gel with sponge were obtained by the reconstruction of many micro-images.

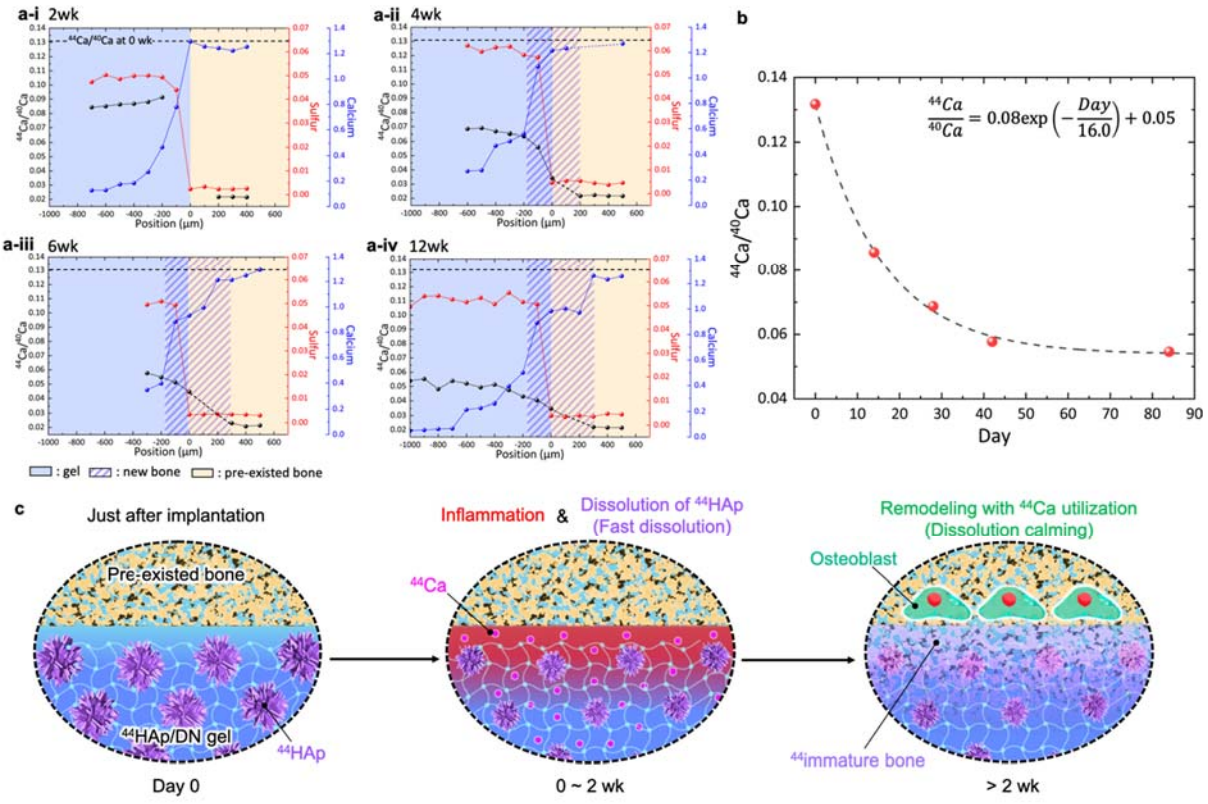

Figure 3. (a) Line profiles of $^{44}Ca/^{40}Ca$ ratio measured by isotope microscopy, normalized sulfur and calcium intensities measured by EDS. The origin of position is defined as the position that sulfur intensity is dramatically dropped to zero. Blue, orange and hatched purple are gel, pre-existed bone and new bone regions, respectively. The dash line parts in the curves of $^{44}Ca/^{40}Ca$ are drawn based on the reference to the line profiles generated from mapping image (Fig. S2). **(b)** Chronological change of $^{44}Ca/^{40}Ca$ ratio at the subsurface of ^{44}HAp-coated DN gel. The characteristic decay time of $^{44}Ca/^{40}Ca$ is 16.0 days that are close to the period of woven bone formation (~2wk). R^2 of the fitting curve was 0.999. **(c)** Schematic illustrations of the primary bone remodeling with ^{44}HAp/DN gel implant according to the results of Figure 3(a) and 3(b). Because the implanted environment just after surgery is acidic due to inflammation, the ^{44}HAp is rapidly dissolved to calcium ions and phosphate ions, and these ions diffuse, partially into bone regions, as revealed in Figure 3(b). After two weeks, the inflammation calms and the immature bone is generated by osteoblasts, utilizing the dissolved ^{44}Ca ions, as revealed

byFigure 3(a). The formation of ^{44}immature bone act as a physical barrier to ion diffusion, which prevents decrement of $^{44}Ca/^{40}Ca$ at later time as revealed in Figure 3(b).

The table of contents

T. Nonoyama*, L. Wang, M. Tsuda, Y. Suzuki, R. Kiyama, K. Yasuda, S. Tanaka, K. Nagata, R. Fujita, N. Sakamoto, N. Kawasaki, H. Yurimoto, J. P. Gong*

Isotope Microscopic Observation of Osteogenesis Process Forming Robust Bonding of Double Network Hydrogel to Bone

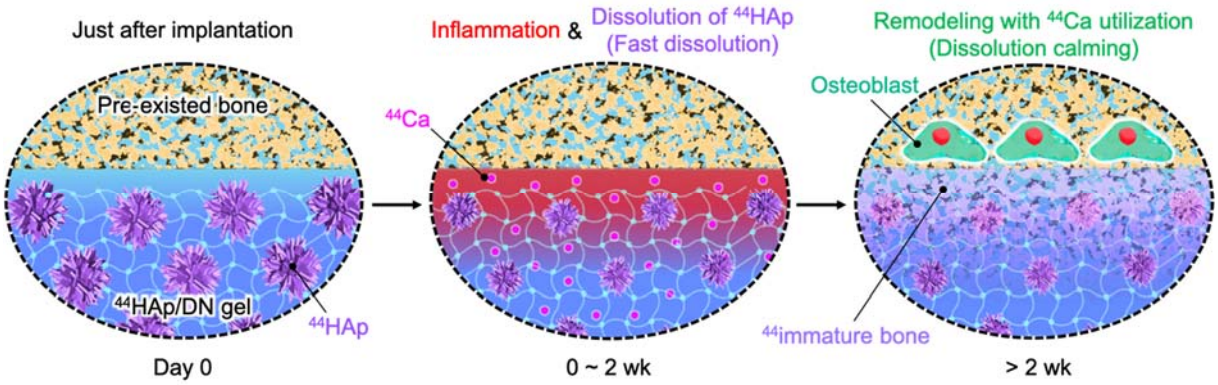

The ^{44}calcium isotope-doped HAp/DN hydrogel was implanted in a defect of rabbit femoral bone, and the dynamic osteogenesis process at the gel/bone interface was traced by the calcium isotope ratio $^{44}Ca/^{40}Ca$ using an isotope microscopy. It is revealed that the osteogenesis penetrates into the DN hydrogel re-utilizing dissolved HAp to form robust bonding.

((Supporting Information can be included here using this template))

Supporting Information

Isotope Microscopic Observation of Osteogenesis Process Forming Robust Bonding of Double Network Hydrogel to Bone

Takayuki Nonoyama[1,2], Lei Wang[2,3], Masumi Tsuda[2,3,5], Yuki Suzuki[4], Ryuji Kiyama[4], Kazunori Yasuda[1,2], Shinya Tanaka[2,3,5], Kousuke Nagata[6], Ryosuke Fujita[7,8], Naoya Sakamoto[7], Noriyuki Kawasaki[6], Hisayoshi Yurimoto[6,7], Jian Ping Gong[1,2,5]**

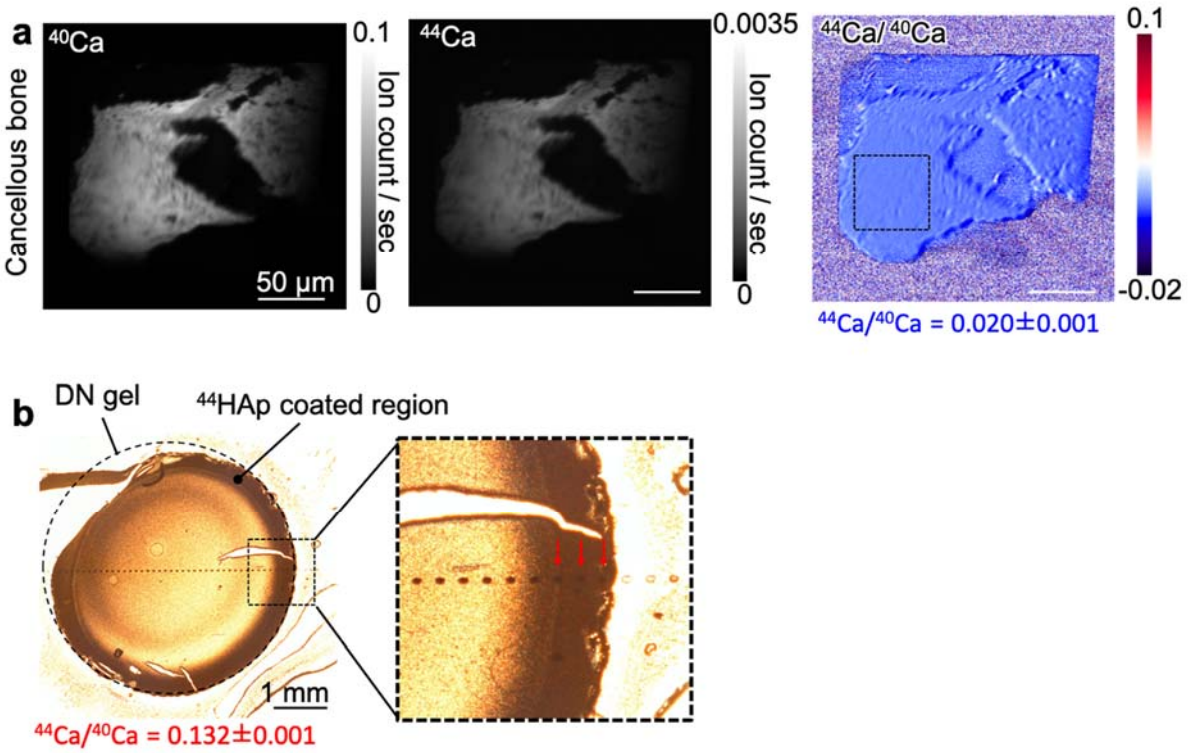

Figure S1. (a) Isotope microscopic images of ^{40}Ca, ^{44}Ca and $^{44}Ca/^{40}Ca$ of the cancellous bone taken at a position far from the implanted HAp/DN gel. The black dotted area in the $^{44}Ca/^{40}Ca$ image was used to estimate the $^{44}Ca/^{40}Ca$ ratio. **(b)** Optical microscopic image of spot measurement of ^{44}HAp/DN gel slice. The horizontal dots were the history of spot measurements. The three dots at the HAP/DN gel hybridized layer shown by red arrows were used to calculate the isotope ratio.

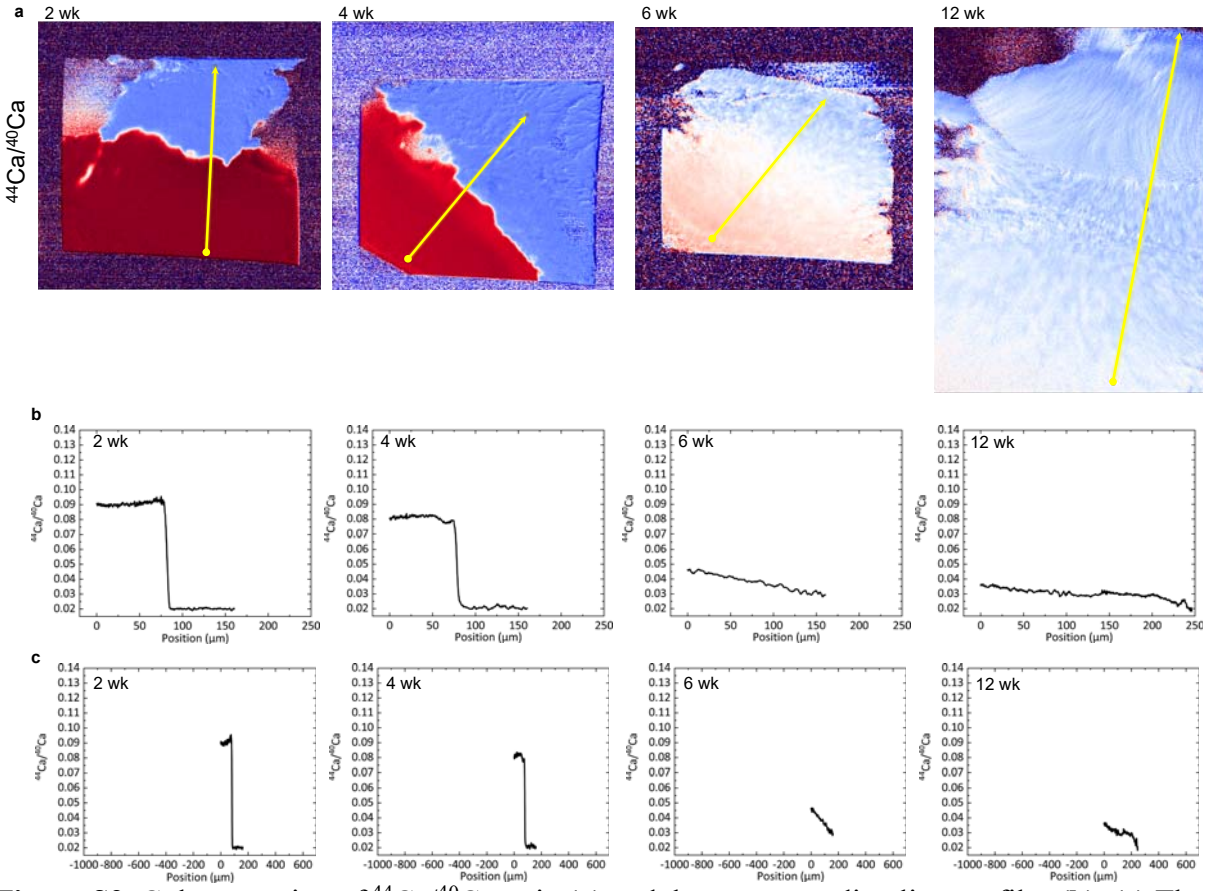

Figure S2. Color mapping of $^{44}Ca/^{40}Ca$ ratio **(a)** and the corresponding line profiles **(b)**. **(c)** The line profiles of **(b)** plotted in the same scale with that in **Figure 3a** for comparison, and the position in the horizontal axis is arbitrary. The tendencies of $^{44}Ca/^{40}Ca$ line profiles generated from imaging data (**Figure S2c**) were almost consistent with those of spot analysis (**Figure 3a**). The 4wk profile was slightly different from those of **Figure 3a** due to different measurement positions.

Materials & Methods

1.Materials

2-Acrylamido-2-methyl propanesulphonic acid (AMPS) was provided by Toagosei Co. Ltd. (Tokyo, Japan). Dimethylacrylamide (DMAAm), *N,N'*-methylenebisacrylamide (MBAA), 2-oxoglutaric acid (α-keto), regular calcium chloride ($^{nat}CaCl_2$), dipotassium phosphate (K_2HPO_4), and tris(hydroxymethyl)aminomethane (Tris) were purchased from Fujifilm Wako Pure Chemical Industries, Ltd. (Osaka, Japan). ^{44}Calcium chloride (isotopic composition: **^{40}Ca 2.89%**, ^{42}Ca 0.06%, ^{43}Ca 0.03%, **^{44}Ca 97.00±0.2%**, ^{46}Ca<0.002%, ^{48}Ca 0.02%) was purchased from Trace Sciences International Corp. (Ontario, Canada). Optimal cutting temperature (O.C.T.) compound and plastic mold for freezing specimen was purchased from Sakura Finetek Japan Co., Ltd. (Tokyo, Japan). Cryo-support film was purchased from Leica Biosystems GmbH (Wetzlar, Germany). A silicon wafer for a substrate of the specimen was purchased from The Nilaco Corporation (Tokyo, Japan).

2.Synthesis of DN hydrogel

The PAMPS/PDMAAm DN gel was synthesized using previously reported methods [1,11]. PAMPS gel was obtained by radical polymerization from an aqueous solution containing 1 M AMPS as a monomer, 4 mol% (to monomer) MBAA as a cross-linker, and 0.1 mol% (to monomer) α-keto as an initiator. The solution was injected into a cell consisting of a pair of glass plates separated by a silicone rubber. The PAMPS gel was synthesized by irradiating the

cell with a UV lamp (wavelength 365 nm) for about 8 h. The obtained PAMPS hydrogel (first network) was then immersed in an aqueous solution containing 2 M DMAAm, 0.1 mol% (to monomer) MBAA, and 0.1 mol% (to monomer) 2-oxoglutaric acid for 1 day until reaching equilibrium. The sample was sandwiched between two glass plates, and the second network (PDMAAm) was subsequently polymerized in the presence of the PAMPS hydrogel by irradiating with UV light for 6 h. After polymerization, the PAMPS/PDMAAm DN gel was immersed in pure water for 1 week, and the water was changed twice daily to remove any unreacted chemicals.

3. ^{44}Ca doped HAp (^{44}HAp) nano-particles mineralization in DN hydrogel

To form the ^{44}Ca doped HAp (^{44}HAp) /DN layer, the DN gel was first immersed in 1 M Tris buffer (pH 9.0) to adjust the pH within the hydrogel because HAp is the most stable in an aqueous solution at pH 9. The gel was then dipped in 300 mM K_2HPO_4 aq for 110 sec, distilled water for 10 sec, 500 mM $CaCl_2$ aq consisting of 450 mM $^{nat}CaCl_2$ and 50 mM $^{44}CaCl_2$ for 110 sec, and distilled water for 10 sec. This alternative dipping process was repeated for 5 cycles to mineralize ^{44}HAp. After the alternative dipping, the hydrogels were dipped in 500 mM $CaCl_2$ aqueous solution containing 10 mol% $^{44}CaCl_2$ (pH 11.0) at body temperature for 24 h to ripen the mineralized amorphous calcium phosphate (ACP) and metastable calcium phosphate crystals to low crystalline HAp. Subsequently, a hybridized HAp/DN layer was formed on the surface of the DN gel. The mineralized layer was approximately 500-μm thick. Considering the natural isotope ratio of calcium (^{40}Ca: 96.94%, ^{44}Ca: 2.086%) and purity of ^{44}Ca isotope reagent, the $^{44}Ca/^{40}Ca$ of the ^{44}HAp on the surface of DN gel is simply estimated as follows,

$$^{44}\mathrm{Ca}/^{40}\mathrm{Ca} = \frac{2.086\% \times \frac{9}{10} + 97.00\% \times \frac{1}{10}}{96.94\% \times \frac{9}{10} + 2.89\% \times \frac{1}{10}} = 0.132$$

4. Surgery

4.1. Animals

Animal experiments were carried out at the Institute of Animal Experimentation at Hokkaido University according to the Rules and Regulations of the University's Animal Care and Use Committee. Total of 4 mature female Japanese White rabbits, weighing 4.0 ± 0.5 kg, were used in this study. The operation for each animal was performed under intravenous anesthesia (pentobarbital, 25 mg/kg) and sterile conditions. Due to the high costs of $^{44}CaCl_2$ isotope chemical and isotope microscopy, one rabbit per each implantation period was used. The evidence of robust bonding of HAp/DN gels to rabbit bone tissues was well-confirmed in our previous reports [11-13].

4.2. Implantation of ^{44}HAp/DN in osteochondral defect

To prepare a specimen of isotope microscopy, we prepared cylindrical DN gel rods (4.5 mm in diameter and 10 mm in height). The surface layer of the rods was mineralized with ^{44}HAp. Then, a 4-mm-high cylindrical plug without HAp coating at its top and bottom was created by cutting a section from the cylindrical rod.

An osteochondral defect (4.3 mm in diameter and 4 mm depth) was created in the femoral groove of the bilateral patellofemoral joints. A 4-mm-high cylindrical plug having plain HAp coating was implanted in the opposite knee as a control. All the rabbits were sacrificed by pentobarbital injection at 2, 4, 6 and 12 weeks after the surgery.

5. Isotope imaging

5.1. Specimen preparation

The harvested rabbit femur with ^{44}HAp/DN implant was cut into 1.5-cm cube. The sample was embedded in the O.C.T. cryo-compound in plastic mold, and then gently frozen in liquid nitrogen pool. The slices (14 μm-thick) of middle part of ^{44}HAp/DN plug with rabbit bone were prepared using the cryostat (Leica CM 3050S, Leica Biosystems GmbH, Wetzlar, Germany), and transferred on cryo-support film. After the slices were completely dried, the films were fixed on a flat silicon wafer by the double-sided carbon tape. Finally, the gold coating treatment on the surface of specimen was applied by physical vapor deposition (Quick Cool Coater SC-701MC, Sanyu electron Co., Ltd., Tokyo, Japan). The low magnification optical images of specimens were acquired by optical microscopy (Nikon Eclipse E600 POL, Nikon Instech Co., Ltd., Tokyo, Japan), and the acquired raw images were merged to make a panoramic image by the photo-merge processing of Photoshop CC 2014 (Adobe, Systems Incorporated, California, US). The slices from the middle position of the cylindrical gel plug were used for analysis.

5.2. Isotope microscopy

The Hokkaido University isotope microscope system, a Cameca ims-1270 secondary ion mass spectrometer (SIMS) equipped with a stacked CMOS-type active pixel sensor (SCAPS), was applied to visualize ^{44}Ca/^{40}Ca distributions on the sample surface [15]. For two-dimensional isotope imaging, an $^{16}O^-$ primary beam of 23 keV was irradiated on the sample surface of approximately 200 × 200 μm^2 with beam currents ranging from c. 20 to 40 nA. The positive secondary ion images of $^{40}Ca^+$ and $^{44}Ca^+$ on the sample surface were collected by the SCAPS detector, with exposure times ranging between 15 and 100 seconds after pre-sputtering for cleaning of the sample surface. The spatial resolution of the Ca isotope images was about 1 μm. For line and spot analyses, an $^{16}O^-$ primary beam of 23 keV and 50 nA was focused on the sample surface of ~30 μm diameter. The positive secondary ions of $^{40}Ca^+$ and $^{44}Ca^+$ were simultaneously collected for 30 s in each spot by two Faraday cups in the multi-collection mode.

6. Energy dispersed X-ray spectroscopy

The quantitative analysis of sulfur and calcium elements of the same samples was performed by spot scanning of energy dispersed X-ray spectroscopy on a scanning electron microscope (JEOL JSM-6010LA, Japan) with energy dispersed X-ray spectrometer (EDS, EX-94400T4L11). The condition of imaging was 20 kV of acceleration voltage, 60 nm of spot size, 10 mm of working distance, 100 sec of duration, and 70 of magnification. The intensities of sulfur and calcium were normalized by that of zinc oxide as a standard sample. ZAF correction (Z: atomic number correction, A: absorbance correction, F: fluorescence correction) was applied to quantitate the obtained data on the software.

7. Statistical analysis

The mean and standard deviation of isotope ratio ^{44}Ca/^{40}Ca in selected area were calculated by using imageJ ver. 1.52q. For Figure 2, the area and number of data point were 10*10 pixels and 100, respectively. In Figure S1a, area and number of data point were 140*140 pixels and 19,600, respectively. Due to the spot analysis, in the calculation of the isotope ratio in Figure S1b, three data points in the right edge of HAp coated region were used.